

A new way to measure cirrus cloud ice water content by using ice Raman scatter with Raman lidar

Zhien Wang

Goddard Earth Sciences and Technology (GEST) Center, University of Maryland Baltimore County, Baltimore, Maryland, USA

Mesoscale Atmospheric Processes Branch, NASA/GSFC, Greenbelt, Maryland, USA

David N. Whiteman and Belay B. Demoz

Mesoscale Atmospheric Processes Branch, NASA/GSFC, Greenbelt, Maryland, USA

Igor Veselovskii

Goddard Earth Sciences and Technology (GEST) Center, University of Maryland Baltimore County, Baltimore, Maryland, USA

Mesoscale Atmospheric Processes Branch, NASA/GSFC, Greenbelt, Maryland, USA

Received 16 March 2004; revised 14 June 2004; accepted 6 July 2004; published 4 August 2004.

[1] To improve our understanding of cirrus cloud radiative impact on the current and future climate, improved knowledge of cirrus cloud microphysical properties is needed. However, long-term studies of the problem indicate that accurate cirrus cloud measurements are challenging. This is true for both, remote sensing as well as in situ sampling. This study presents a new method to remotely sense cirrus microphysical properties utilizing the Raman scattered intensities from ice crystals using a Raman lidar. Since the intensity of Raman scattering is fundamentally proportional to the number of molecules involved, this method provides a more direct way of measuring the ice water content compared with other schemes. Case studies presented here show that this method has the potential to provide simultaneous measurements of many of the essential information of cirrus microphysical properties.

INDEX TERMS: 0320 Atmospheric Composition and Structure: Cloud physics and chemistry; 0394 Atmospheric Composition and Structure: Instruments and techniques; 3360 Meteorology and Atmospheric Dynamics: Remote sensing.
Citation: Wang, Z., D. N. Whiteman, B. B. Demoz, and I. Veselovskii (2004), A new way to measure cirrus cloud ice water content by using ice Raman scatter with Raman lidar, *Geophys. Res. Lett.*, 31, L15101, doi:10.1029/2004GL020004.

1. Introduction

[2] Cirrus clouds affect the surface and top-of-atmosphere energy budgets and can produce large local variations in atmospheric heating. The degree and extent of the so-called greenhouse-versus-albedo effects involving cirrus clouds will lead to significant atmospheric differential cooling and heating in the vertical as well as on horizontal scales [Liou, 1986] and is dependent on cirrus microphysical properties and their vertical distribution [Stephens *et al.*, 1990]. However, it is a challenging task to measure cirrus Ice Water Content (IWC) and particle size by remote sensing or in situ sampling. IWC estimated from in situ

particle size probes has large uncertainties associated with different ice crystal shapes and densities [Heymsfield *et al.*, 2002]. There have been significant advances in ground-based remote sensing of cirrus clouds using the Department of Energy Atmospheric Radiation Measurement (ARM) program Cloud and Radiation Testbed (CART) site measurements [Mace *et al.*, 1998; Wang and Sassen, 2002]. Nevertheless, uncertainty in the retrieved IWC by using lidar, radar, and radiometer measurements might be very large under some situations because one has to make several critical assumptions about cirrus clouds such as the size distribution and density of ice crystals, which vary a lot in cirrus clouds. A remote sensing method that possesses a signal that is directly related to IWC would be very attractive for IWC measurements and would also be of great value in studying other techniques for obtaining IWC. Here, we report on a new method to remotely measure IWC using Raman scattering from ice in cirrus clouds. First, we briefly describe our Raman lidar system. Then we present the method and measurements. Results from a lidar-radar algorithm are used to calibrate the ice Raman scatter based retrieval algorithm.

2. The GSFC Scanning Raman Lidar (SRL)

[3] The GSFC/NASA SRL uses a tripled Nd:YAG laser (355 nm) combined with two telescopes using different fields of view to measure high altitude and low altitude signals. Light backscattered by molecules and aerosols at the laser wavelength as well as Raman scattered light from water vapor (3657 cm^{-1}), liquid/solid water (3200 cm^{-1} to 3600 cm^{-1}), and nitrogen (2329 cm^{-1}) molecules is collected by a 0.76 m, $f/5.2$, variable field-of-view Dall-Kirkham telescope mounted horizontally on a 3.7 m optical table. This telescope is typically operated using 0.25-milliradian field of view and acquires the high altitude signals. A smaller 0.25 m telescope is mounted inside of the larger telescope and operates at ~ 1.0 milliradian field of view. Figure 1 presents the transmission of solid/liquid water and water vapor filters used in SRL along with the water and ice Raman scatter spectrum at the laser wavelength of 355 nm

[Bunkin *et al.*, 2000]. Although the solid/liquid filter was designed for liquid water measurements, it is still capable to measure $\sim 70\%$ of the ice Raman scatter signal. Therefore, this filter can provide measurements for both liquid and solid water.

3. The Method

[4] The radiant flux of the Raman scattering from the chemical substance A in bulk material is given by [Tobin, 1971]:

$$F_{R,A} = F_0 c_A N_a V \sigma_A(\nu_0, \nu_s, T, c_i), \quad (1)$$

Where F_0 is the radiant flux density of the incident laser beam, c_A is the molar concentration of component A , N_a Avogadro's number, and V the probed volume. The scattering cross section σ_A depends on the frequency of the laser ν_0 , the frequency of the scattered radiation ν_s , and on the temperature T of the sample in general.

[5] Because temperature changes usually alter the intermolecular forces in liquid or solid substances, the shape of the Raman spectrum is dependent on temperature. The common features are a broadening of the Raman lines with increase in temperature accompanied by a shift of the Stokes lines to higher frequencies [Loudon, 2001; Scherer and Snyder, 1977]. The shifts of ice Raman spectrum among different types of ices have been observed because of crystalline differences. According to the ice phase diagram, all of the natural ice on earth is Ice Ih (hexagonal ice). This type of ice does not show large changes in the spectrum at atmospheric temperatures, therefore the shift of the ice Raman spectrum with temperature in cirrus clouds is expected to be moderate. However, the temperature dependence can be accounted for in the data analysis, and be minimized by using a wide filter to cover the whole ice Raman spectrum.

[6] For ice crystal study, equation (1) can be reformatted as [Vehring *et al.*, 1998]:

$$F_{R,A} = C F_0 IWC M V \sigma_A(\nu_0, \nu_s, T), \quad (2)$$

Where C is a constant and IWC is ice water content ($C IWC = c_A N_a$). The morphology factor M is introduced, and M is a possible function of the orientation, the size and the shape of the ice crystals for a given laser frequency. In lidar measurements, the Raman signal is integrated over a large

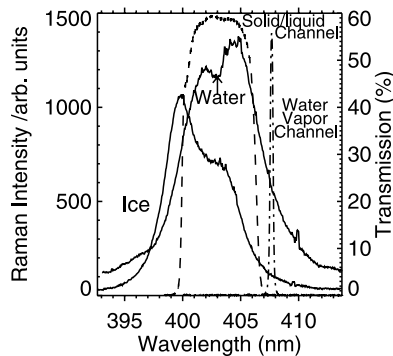


Figure 1. Water and ice Raman scatter spectrum and the transmission of solid/liquid and water vapor filters used in SRL.

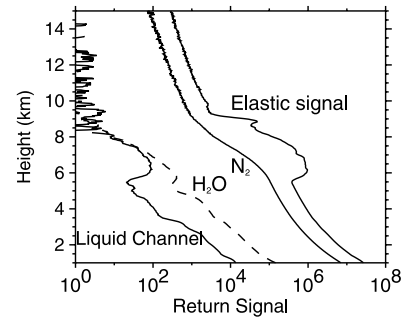


Figure 2. An example of SRL signals (10-min average) measured on 12 November 2003 at the SGP CART site. Note that different channels: elastic channel (*elastic signal*), nitrogen Raman channel (N_2), water vapor Raman channel (H_2O), and solid/liquid water Raman channel (*liquid channel*).

volume temporally and spatially. Raman scattering intensity is fundamentally proportional to the number of molecules in the probed volume implying that lacking any resonance phenomena due to ice crystal morphology or non-random orientation, the M for randomly oriented ice crystals should be a constant. Furthermore, several experimental studies indicated that the Raman scatter from droplets with size parameters ($2\pi r/\lambda$) larger than 60 is proportional to the volume of droplets if averaged over a small parameter range. Therefore, we regard M as a constant for the first order approximation.

[7] Based on above discussion, the lidar equation of ice Raman scatter can be expressed as

$$P_{ice}(R) = \frac{C_{ice} P_0 IWC \sigma_{ice}(\nu_0, \nu_{ice}, T)}{R^2} \times \exp\left(-\int_0^R (\alpha(\nu_0, r) + \alpha(\nu_{ice}, r)) dr\right), \quad (3)$$

where P_{ice} is return power at the ice Raman scatter frequency ν_{ice} , P_0 is transmitted laser power, and R is the range from lidar station. C_{ice} is a new constant including lidar system constant and constants of C and M in equation (2). $\alpha(\nu_0, r)$ and $\alpha(\nu_{ice}, r)$ represent atmospheric extinction coefficients including the scatter and absorption of molecules and particles at frequencies ν_0 and ν_{ice} and range r , respectively.

[8] For the Raman scatter of nitrogen, we have

$$P_{N_2}(R) = \frac{C_{N_2} P_0 N_{N_2}(R) \sigma_{N_2}(\nu_0, \nu_{N_2}, T)}{R^2} \times \exp\left(-\int_0^R (\alpha(\nu_0, r) + \alpha(\nu_{N_2}, r)) dr\right), \quad (4)$$

where N_{N_2} is the number density of nitrogen at range R and ν_{N_2} is the Raman scatter frequency of nitrogen.

[9] Combining equations (3) and (4), we have

$$IWC = \frac{P_{ice}(R)}{P_{N_2}(R)} \frac{C_{N_2} N_{N_2}(R) \sigma_{N_2}(\nu_0, \nu_{N_2}, T)}{C_{ice} \sigma_{ice}(\nu_0, \nu_{ice}, T)} \times \exp\left(-\int_0^R (\alpha(\nu_{N_2}, r) - \alpha(\nu_{ice}, r)) dr\right), \quad (5)$$

On the right side of this equation, $P_{ice}(R)/P_{N_2}(R)$ is known from lidar measurements; $(C_{N_2} N_{N_2}(R) \sigma_{N_2}(\nu_0, \nu_{N_2}, T)/$

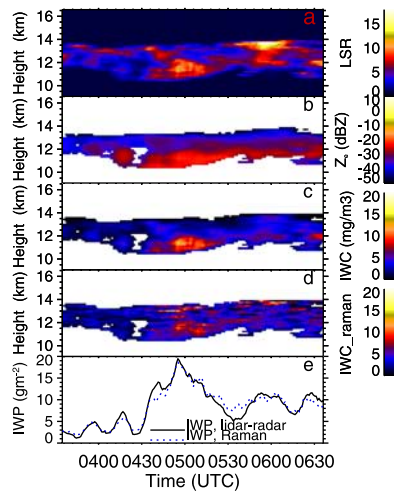


Figure 3. Time-height display of lidar scattering ratio (a), radar reflectivity factor (Z_e , b), IWC from the lidar-radar algorithm (c), IWC using ice Raman signal (d), and the intercomparison of IWP derived from these two methods (e) observed at the SGP CART Site on 31 October 2003.

($C_{ice} \sigma_{ice}(v_0, v_{ice}, T)$) can be approximated as $K(T) \beta(R)$, where $K(T)$ is a new constant and $\beta(R)$ is backscattering coefficient of molecules; the exponential term represents the difference of atmospheric attenuation difference at the two Raman channels. K might slightly depend on temperature, but we neglect the temperature dependency in this study. Based on these discussions, equation (5) can be expressed as:

$$IWC = \frac{P_{ice}(R)}{P_{N_2}(R)} K \beta(R) \times \exp\left(-\int_0^R (\alpha(v_{N_2}, r) - \alpha(v_{ice}, r)) dr\right), \quad (6)$$

Therefore, we only need to know K to determine IWC from SRL measurements, and an approach to determine K is presented below.

[10] With retrieved IWC and estimated extinction coefficient from Raman lidar measurements, general effective size (D_{ge}) can be estimated by using relationship of $\alpha = IWC (-2.93599 \times 10^{-4} + 2.54540/D_{ge})$ developed by *Fu* [1996]. Units for α , IWC , and D_{ge} are m^{-1} , $g m^{-3}$, and μm , respectively. When K is known, we obtain IWC and D_{ge} profiles from SRL measurements.

4. Measurements

[11] During the Atmospheric Infrared Sounder (AIRS) Water Vapor Experiment-Ground (AWEX-G) between 27 October and 16 November 2003, the SRL was sited at the ARM Southern Great Plains (SGP) CART site. An

example of SRL signals (10-min average) measured on 12 November is presented in Figure 2. During this time, cirrus clouds were between 6 and 9 km above ground level, with optical depth of ~ 1.2 . The optical depth is calculated from cloud layer transmittance estimated from the clear sky signals of elastic and/or nitrogen channels below and above the cloud layer. A strong signal was measured in the liquid/solid Raman channel in the cirrus layer as indicated by strong backscatter signal in elastic channel and moderate attenuation in the N_2 channel.

[12] As discussed above, we need to know the value of K to estimate IWC . If we know Raman scattering cross-section of ice and nitrogen, the optical transmittance of receiving system, and other system constants, we can calculate K directly. We hope to pursue this work in the future. Here, however, we use an alternative method to determine K by comparing with IWC or ice water path (IWP) derived from a published lidar-radar algorithm [Wang and Sassen, 2002]. The lidar-radar algorithm uses cirrus extinction coefficient and radar reflectivity factor to estimate IWC and D_{ge} . In this algorithm, the accuracy of IWC or IWP mainly depends on the accuracy of extinction coefficient or optical depth. Between extinction coefficient and optical depth derived from Raman lidar measurements, optical depth has better accuracy due to its lower susceptibility to multiple scattering effects [Whiteman et al., 2001]. Therefore, IWP is better than IWC for the intercomparison to calculate the constant K .

[13] The AWEX-G field campaign provided a chance to use this approach to estimate K , and an example is given in Figure 3. Figures 3a and 3b present time-height display of lidar scattering ratio from SRL and radar reflectivity factor (Z_e) from the millimeter cloud radar at the SGP CART Site. To provide cirrus extinction coefficients for the lidar-radar algorithm, we simply multiply cirrus backscattering coefficients with a layer mean extinction-to-backscattering ratio estimated from optical depth and layer-integrated backscattering coefficient [Whiteman et al., 2001]. IWC profiles retrieved from the lidar-radar algorithm are given in Figure 3c. As mentioned above, we use IWP from the lidar-radar algorithm to determine K , and a comparison of IWP time series from the lidar-radar algorithm and from ice Raman signal is given in the Figure 3e, which indicates that they agree well and follow the same pattern of variation. IWC profiles from ice Raman signal are presented in Figure 3d. Comparing Figures 3c and 3d, we see good agreement between the two approaches. However, there are some differences between them, which may be caused by the uncertainties in the lidar-radar retrieval and/or the lower signal-to-noise ratio of Raman signal at some altitudes.

[14] We performed the same calibration procedure on five different cirrus events during the AWEX-G. The results are listed in Table 1. These cases cover a mid-cloud temperature range of -24 to -60 degree with optical depth ranging

Table 1. The Statistics of Cirrus Properties and the K for the Five Cirrus Events During the AWEX

Date	10/30/2003	10/31/2003	11/2/2003	11/4/2003	11/12/2003
Mean Cloud Base and top Heights (km)	10.5, 12.0	11.0, 13.8	11.4, 12.2	10.2, 12.5	6.0, 9.1
Mean Middle cloud temperature ($^{\circ}C$)	-52.4	-59.2	-51.5	-48.5	-23.8
Mean Optical Depth	0.356	0.736	0.155	0.899	1.225
K	2.975	2.483	1.813	2.756	3.284
IWP correlation coefficient	0.986	0.964	0.950	0.886	0.974

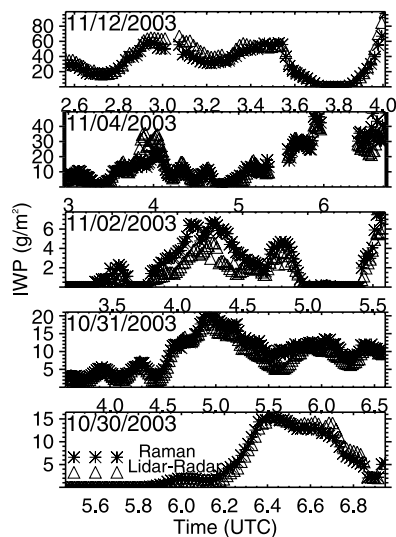


Figure 4. Comparisons of IWPs derived by the lidar-radar algorithm and from ice Raman scatter using a mean K for the five cirrus cloud cases summarized in the Table 1.

from 0.05 to 2. The K calculated from each individual event range from 1.813 to 3.284. The observed variation of K might be caused by uncertainties in IWPs from the lidar-radar algorithm, signal noises in ice Raman signals, and possible dependencies on cloud temperature and particle size and shape. Comparing with the other days, the K on 2 November 2003 has a relatively low value. This is an optically thin cirrus cloud with low Z_e , and there are potential larger errors in K because of the relatively low signal-to-noise ratio of ice Raman signal and relatively large percentage errors in estimated optical depth and measured Z_e . Excluding this case, K has a mean of 2.875 with a standard deviation of 0.339, which is $\sim 11.8\%$ of the mean. Considering uncertainties in the IWP estimated from the lidar-radar algorithm, the range of variation of K is reasonable and might mainly be caused by these uncertainties. Therefore, we use the mean K to calculate IWC.

[15] Applying the mean K to all cases, we can get IWC and D_{ge} profiles. Comparisons between IWP derived by the lidar-radar algorithm and that from ice Raman scattering are given in Figure 4. In general, there is good agreement between these two methods. The intensity of Raman scattering is fundamentally proportional to the number of molecules involved, though the shape of the spectrum is dependent on temperature. The change of the transmitted ice Raman intensity over a range of 40 degree is expected to be less than 5%. Therefore, it is reasonable to assume that K is the essentially constant during the AWEX-G field campaign because the same optical configuration was used for the entire mission. Then, the periods when the two IWPs do not follow each other well might indicate potential errors in the lidar-radar method because of possible failures of assumptions in the algorithm or errors in the inputs. This figure shows a potential to use Raman IWC measurements to refine other remote sensing methods.

5. Conclusions

[16] This paper presented a new approach to remotely sense IWC and D_{ge} using the ice Raman signal observed by

a Raman lidar. As demonstrated in the case studies, this method provides the essential information of cirrus microphysical properties to study cloud physical processes in cirrus clouds. The main limitation of this method is the weak ice Raman signal which limits measurements to nighttime only. Nonetheless, the signal presented in this paper can be improved a lot. First, it can be improved by optimal design of the filter to include main ice Raman scattering spectrum. In the current SRL, the filter was optimized for liquid water measurements. Second, it can be improved by increasing transmitted laser power. The laser power for measurements presented in this paper is only about 7 W. With improvements such as these, increases in signal to noise of between 2–4 can be expected. Therefore, Raman lidar might be an effective tool to measure IWC and D_{ge} for cirrus cloud study during nighttime, though it only can provide them for part of optically thick ice clouds. A Raman lidar operated from an aircraft, such as the NASA/GSFC Raman Airborne Spectroscopic Lidar (RASL at <http://ramanlidar.gsfc.nasa.gov>), might provide an effective alternative method for in situ IWC measurements with much large sampling volume than other approaches. To further improve the accuracy of the method, we will study the temperature dependence of ice Raman scattering cross-section.

[17] **Acknowledgments.** This research has been partly supported by NASA and DOE grant DE-FG02-03ER63536 from the Atmospheric Radiation Measurement Program. We thank Dr. Bunkin at General Physics Institute, Russian Academy of Sciences for providing us Raman spectra data of ice and water.

References

- Bunkin, A. F., G. A. Lyakhov, N. V. Suyazov, and S. M. Pershin (2000), Sequence of water thermodynamic singularities in Raman spectra, *J. Raman Spectrosc.*, *31*, 857–861.
- Fu, Q. (1996), An accurate parameterization of the solar radiative properties of cirrus clouds for climate models, *J. Clim.*, *9*, 2058–2082.
- Heymsfield, A. J., S. Lewis, A. Bansemir, J. Iaquinta, L. M. Miloshevich, M. Kajikawa, C. Twohy, and M. R. Poellot (2002), A general approach for deriving the properties of cirrus and stratiform ice cloud particles, *J. Atmos. Sci.*, *59*, 3–29.
- Liou, K. N. (1986), Influence of cirrus clouds on weather and climate processes: A global perspective, *Mon. Weather Rev.*, *114*, 1167–1199.
- Loudon, R. (2001), The Raman effect in crystals, *Adv. Phys.*, *50*, 813–864.
- Mace, G. G., T. A. Ackerman, P. Minnis, and D. F. Young (1998), Cirrus layer microphysical properties derived from surface-based millimeter radar and infrared interferometer data, *J. Geophys. Res.*, *104*, 16,741–16,753.
- Scherer, J. R., and R. G. Snyder (1977), Raman intensity of single crystal ice I_h , *J. Chem. Phys.*, *67*, 4794–4811.
- Stephens, G. L., S. C. Tsay, P. W. Stackhouse, and P. J. Flatau (1990), The relevance of the microphysical and radiative properties of cirrus clouds to climate and climatic feedback, *J. Atmos. Sci.*, *47*, 1742–1753.
- Tobin, M. C. (1971), Laser Raman spectroscopy, in *Chemical Analysis*, edited by P. J. Elving and I. M. Kolthoff, 184 pages, John Wiley, Hoboken, N. J.
- Vehring, R., C. L. Aardahl, G. Schweiger, and E. J. Davis (1998), The characterization of fine particles originating from an uncharged aerosol: Size dependence and detection limits for Raman analysis, *J. Aerosol Sci.*, *29*, 1045–1061.
- Wang, Z., and K. Sassen (2002), Cirrus cloud microphysical property retrieval using lidar and radar measurements: I. Algorithm description and comparison with in situ data, *J. Appl. Meteorol.*, *41*, 218–229.
- Whiteman, D. N., et al. (2001), Raman lidar measurements of water vapor and cirrus clouds during the passage of Hurricane Bonnie, *J. Geophys. Res.*, *106*, 5211–5225.

B. B. Demoz and D. N. Whiteman, Mesoscale Atmospheric Processes Branch, Code 913, NASA/GSFC, Greenbelt, MD 20771, USA.

I. Veselovskii and Z. Wang, GEST Center, University of Maryland Baltimore County, Code 912, NASA/GSFC, Greenbelt, MD 20771, USA (zhien@agnes.gsfc.nasa.gov)